Special Conference Edition, April, 2022

http://dx.doi.org/10.4314/bajopas.v13i1.69S

Bayero Journal of Pure and Applied Sciences, 13(1): 455 - 466
ISSN 2006 – 6996

INTERPRETATION ANALYSIS FROM SATELLITE GRAVITY DATA TO IMAGE THE UPPER LITHOSPHERIC PATTERNS AND THEIR HYDROCARBON SIGNIFICANCE IN SOKOTO BASIN, NIGERIA

Adamu, A[a*]. Likkason, O.K[b]., Maigari, A.S[c]., Ali, S[b]. and Yohanna, A[d]
[a*]Department of Applied Geophysics, Federal University Birnin Kebbi, Nigeria
[b]Department of Physics, Abubakar Tafawa Balewa University Bauchi, Nigeria
[c]Department of Applied Geology, Abubakar Tafawa Balewa University Bauchi, Nigeria
[d]Department of Geology, Federal University of Lafia, Nasarawa, Nigeria
[a*]Correspondence's author's email: adamu.abubakar35@fubk.edu.ng
http://orcid.org/0000-0002-8902-7458

ABSTRACT
Meaningful exploration and comprehensive geological evidence have been made by the analyses of satellite gravity data for defining the basin's tectonic framework, subsurface structures as well as delineating favourable regions of hydrocarbon prospect for further appraisal. A digitized composite satellite gravity data covering some parts of Sokoto Basin were acquired and processed to interpret the Bouguer anomalies over the area and to equally image the upper lithospheric patterns beneath the Sokoto Basin and its surroundings. We aim to understand the structural styles of crustal extension in some parts of the Sokoto Basin. Regional and residual gravity components, these were obtained by least-square fitting of a third-degree order polynomial surface to the Bouguer anomaly. The residual anomalies feature NE-SW gravity lows attributed to sedimentary in-fill about the localities of Argungu, Yauri, Koko and Jega, Kamba, Bagudo, Tambuwal, Goronyo, Gada as well as Kolmalo. Data enhancement techniques such as first vertical derivative, total horizontal derivative (THDR), analytic signal, spectral depth analysis, and the standard Euler deconvolution (SED) were applied to enhance deep-seated structures. Results from the qualitative analysis of spectral depth revealed that the average thickness of the sediments varies from 1.679 km to 4.181 km, outsized enough for hydrocarbon prospect. The derivative maps revealed parallel to sub-parallel trending NW-SE, E-W fracture zones within the sedimentary in-fill underlying the study area, coinciding with the cretaceous zones. Hence, the identified lineaments (faults or lithologic contacts) and structures in the area can be attributed to the tectonic setting of the area and probable migratory routes for hydrocarbon migration. More detailed ground gravity and seismic studies may lead to discoveries of structural or stratigraphic traps. We conclude that the area is a promising prospect in terms of oil and gas prospecting.
Keywords: Enhancement filtering techniques, Structural mapping, Satellite gravity data, Sokoto Basin

INTRODUCTION

The Sokoto Basin which covers Zamfara, Sokoto and Kebbi States of Nigeria has drawn the attention of geoscientists and stake-holders in the petroleum industry largely because of intensified petroleum exploration efforts in the inland basins and the fact that Nigeria's Department of Petroleum Resources has identified the Sokoto Basin as one the potential hydrocarbon-bearing inland basins. There is equally another compelling reason for the exploration efforts in the Sokoto Basin (Kogbe, 1972, 1979, 1981; Obaje *et al.,* 2009, 2020). Commercial deposits of oil and gas have been discovered and are being produced from contiguous structurally and stratigraphically rifted basins of the Niger Republic, Chad Republic, Sudan, Burkina-Faso and Mali. The potential field gravity method has proved very effective for providing useful information known to guide various exploration campaigns, be it regional studies (Olawale *et al.,* 2020; Ali *et al.,* 2016; Marwan and Yahia, 2018; Hesham and Oweisi, 2016; Augustine *et al*., 2020), economic mineral or oil and gas exploration (Mohamed *et al.* 2016; Charles *et al.,* 2020; Kebede and Mammu, 2021).

Meaningful exploration and comprehensive geological information have been made by the analyses of satellite gravity data for defining the basin's tectonic framework, subsurface structures as well as delineating favourable regions of hydrocarbon prospect for further appraisal (Marwan & Yahia, 2018; Augustine *et al.,* 2020; Ghosh, 2016; Mohamed *et al.,* 2016). Gravity survey is the primary method in geophysical exploration as a regional and local structural mapping tool (Reid, 2003; Reid *et al.,* 1990; Reid *et al.,* 2003; Ghosh, 2016). The effectiveness of a gravity survey depends on the existence of significant density contrast between altered rocks or structures and their host rocks. Moreover, the gravity survey not only reflects the shape of major granitoid, but also a correspondence between the tectonic lineaments and regional fault systems (Ghosh 2016). Therefore, gravity surveying is also useful for searching intrusive bodies and major faults. Nowadays, there are simpler techniques of interpreting gravity data to improve output result and to help an explorer make reasonable decisions. Such techniques include Standard Euler deconvolution (SED), Spectral depth, Analytic signal and Source parameter imaging (Reid, 2003; Ghosh, 2016). The present study is based on analysis, interpretation and mapping of the structural features of acquired satellite gravity data in some parts of Sokoto Basin, northwestern Nigeria, to improve our knowledge of the structural framework of the study area through identification of linear structures and determination of depth to underlying ground subsidence. Information obtained as regards the study area's structural context and sedimentary rock thickness will serve as a guide to mineral and/or hydrocarbon exploration. The study area falls within Sokoto basin and it spans about 29,600 km^2, situated between latitudes 03° 00′ N and 05° 30′ N and longitudes 11° 00′ E and 13° 00′ E (figure. 1).

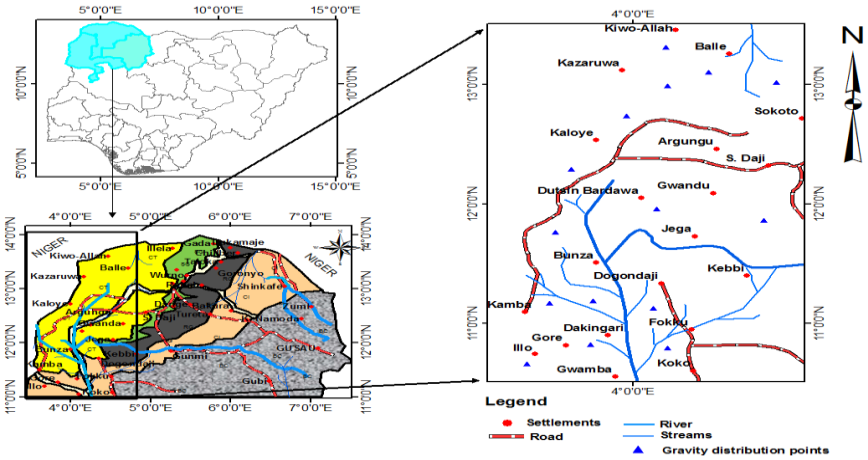

Figure 1: Map of Nigeria Showing the location of Sokoto Basin and "Study Area" respectively (After Petters, 1978; Kogbe, 1979)

Geology of the Sokoto Basin

The Sokoto Basin is predominantly a gently undulating plain with an average elevation varying from 250 m to 400 m above sea level. The plain is occasionally interrupted by low mesas and other escarpment features (Kogbe 1979, 1981 & Obaje 2009). The sediments of the Iullemmeden Basin were thought to accumulate during four main phases of deposition as follows: (figure. 2 & Table 1)

(a) The Illo and Gundumi Formations (made of grits and clays) unconformably overlay the pre-Cambrian Basement Complex. This is the so-called pre-Maastrichtian 'continental interclaire' of West Africa (Obaje *et al.* 2020).

(b) Next on the succession is the Maastrichtian (66 – 72 Ma) Rima Group (consisting of mudstones and friable sandstones (the Taloka and Wurno formations) separated by the fossiliferous, calcareous and shaley Dukamaje Formation overlie the Illo and Gundumi Formations unconformably (Obaje *et al.* 2020).

(c) The Dange and Gamba Formations (mainly shales) separated by the calcareous Kalambaina Formation constituting the Paleocene (56 – 66 Ma) Sokoto Group overlie the Rima Group (Kogbe, 1979).

(d) The sequence cover is the Gwandu Formation of the Eocene (33 – 56 Ma) age forming the continental terminal (Kogbe, 1981).

The sediments dip gently and thicken gradually towards the northwest with maximum thicknesses attainable towards the border with the Niger Republic.

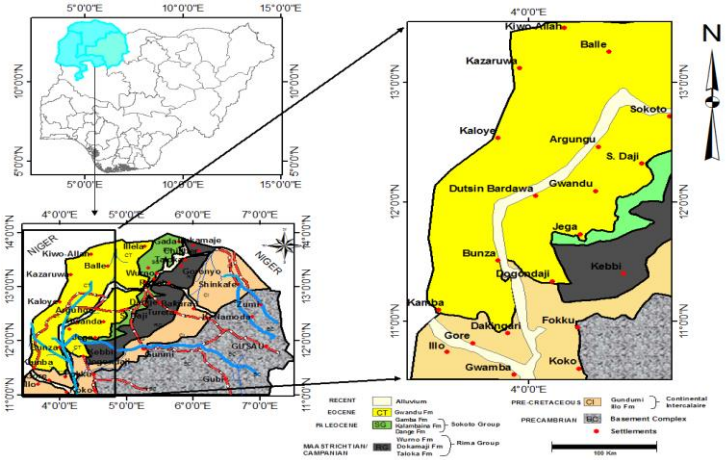

Figure 2: Geological Map of Nigeria Showing the "Sokoto Basin" and the Study Area (Modified After Kogbe, 1978)

Table 1: Stratigraphic successions in the Sokoto Basin (after Obaje *et al.,* 2009)

Age	Type/Group	Formation	Sediment type	Remark
Eocene	-	Gwandu	Continental	Continental Terminal
Paleocene	Sokoto Group	Gamba Kalambaina Dange	Marine Marine Marine	- - -
Maastrichtian	Rima Group	Wurno Dukamaje Taloka	Continental Marine Continental	- - -
Pre-Maastrichtian		Gundumi - Illo	Continental	Continental Intercalaire
Pre-Cambrian	**Basement Complex Rocks**			

MATERIALS AND METHODS

In this present study, satellite gravity data were acquired, analysed, and processed for imaging the upper lithospheric structures underneath the southeastern parts of Sokoto basin. The gravity method depends on the measurements of variations in the gravity field caused by horizontal variations of density in the subsurface (Ismail *et al.,* 2001; Askari, 2014; Mammo, 2004). It is the essential method in several of specific geological studies, as in mapping near-surface voids, quantitative studies of metallic ore bodies, characterizing salt structures, and monitoring changes of fluid/gas content in volcanoes. The gravity method has also been used in the regional characterization of the earth to determine the structures of the crust, identifying potentially favourable regions for resource exploration, and developing conceptual exploration models (Hinze *et al.,* 2013; Tiberi *et al.,* 2005; Saltus & Blakely, 2011).

Theoretical background

Separation of regional-residual field

The anomalous value of the gravity field at a point is the sum of the gravity effects of widespread Jacobsen (1987) demonstrated that if a potential field is upward continued to a certain height z, and deep-seated mass distributions and smaller, localized mass distributions near the observation point. The interpretation of Bouguer gravity anomalies often involves isolating anomalies of interest (residual gravity anomalies) (Mickus *et al.,* 1991; Linser, 1967). The observed Bouguer gravity anomaly field consists of two components: a regional and residual gravity anomaly field. The regional-residual separation process was applied to the gravity data-set to estimate the amplitude of the regional background. The upward continuation can be used to separate a regional gravity anomaly resulting from deep sources from the observed gravity (Kebede *et al.,* 2020; Mammo, 2004; Linser, 1967). This is an operation that shifts the data by a constant height level above the surface of the earth (or the plane of measurements). It is used to estimate the large scale or regional (low frequency or long wave length) trends of the data. Since the target depth is the sedimentary infill which is approximately undulating 1 km – 3 km, the data is upward continued at 5 km to remove the short-wavelength anomalies.

then it is possible to focus on sources situated at a depth greater than z = 2 (see also Lyngsie *et al.,* 2006; Mammo 2004).

The Upward continuation

It is a mathematical technique used to separate the anomaly of the deeper geology from shallower geology (Jacobsen, 1987). It is a transformation of gravity anomaly computed at a point, Q (x_0; y_0; $z_0 = 0$) on the mean sea-level to a point P (x_0; y_0; $z_0 = -h$) on some higher flat surface upward continued to, z = h < 0 (figure. 3). The gravitational attraction per unit mass of an anomalous source body of mass, ***dm***; at mean see level, O (x_0; y_0; $z_0 = 0$) at distance *R* from the source location point Q (x, y, and z) is computed by:

$$dg = \frac{Gdm}{R^2} = \frac{Gdm}{(x-x_0)^2+(y-y_0)^2+(z-z_0)^2} \quad \text{..... (1)}$$

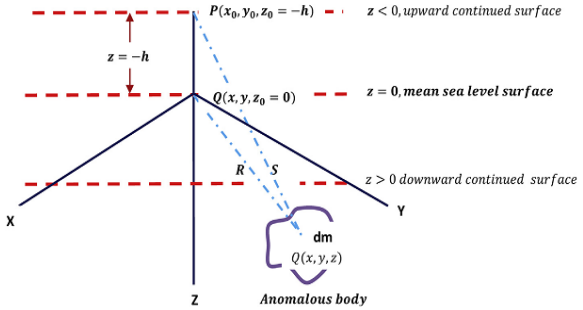

Figure 3. Pictorial representation of upward continuation technique in the Cartesian coordinate system (After Kebede *et al.,* 2020).

The vertical component, dg_z, gives the gravity anomaly, Δg_0, of the source at the mean sea level surface point as;

$$dg_z = \Delta g_0 = \frac{Gdm}{R^2}\frac{z}{R} = Gdm\frac{z}{R^3} = Gdm\frac{z+h}{[(x-x_0)^2+(y-y_0)^2+(z)^2]^{3/2}} \quad \text{..... (2)}$$

Thus the gravity anomaly, Δg_p, of the anomalous source at the upward continued surface point P is:

$$\Delta g_p = \frac{Gdm}{S^2}\frac{z+h}{S} = Gdm\frac{z+h}{S^2} = Gdm\frac{z+h}{[(x-x_0)^2+(y-y_0)^2+(z+h)]^{3/2}} \quad \text{..... (3)}$$

Equation (3) represents the gravitational attraction of ***dm*** at a height, 'h', above the mean sea level surface. This filter attenuates the short-wavelength anomaly components while enhancing the long-wavelength ones. This equation therefore, represents an algorithm for developing an upward Continuation filter.

Satellite Gravity data

The Bouguer gravity anomaly data (Fig. 6) were obtained from the International Gravity Bureau, which maintains the WGM 2012 (Balmino *et al.,* 2011; Zelalem *et al.,* 2018). The WGM 2012 Bouguer gravity anomalies were calculated using the Earth Gravity model, EGM 2008, satellite gravity and the Topography 1 arc-minute (ETOP1) database for topography. This is to provide harmonic coefficients for a spherical harmonic expansion up to an order of 10, 800 to produce the Earth's Topography derived gravity model at 1' x 1' resolution (ETOPG1) model (Balmino *et al.,* 2011; Zelalem *et al.,* 2018).

Edge detection techniques

First vertical derivative (FVD)

This enhancement technique applied on the Bouguer anomaly map is to sharpen up anomalies and allow clearer imaging of the causative structures vertically. The first vertical derivative filtering action is applied to enhance the high-frequency components at the expense of low-frequency components which are deeply seated. The first vertical derivative can also be applied to the gravity data by using the amplitude spectra of the gravity field (Gunn *et al.,* 1997; Reid, 1990). This transformation magnifies the short-wavelength features (Mammo, 2010), which could reflect the residual anomalies. The gridded gravity anomaly data in (figure. 3) can be expressed as a function in the Cartesian co-ordinate system, i.e. F = f(x, y, z). The vertical derivative which shows the change of field with depth (z) is expressed as;

$$FVD = -\left(\frac{\partial f_v}{\partial z}\right) \quad \text{..... (4)}$$

The residual anomalies obtained through subtraction of upward continued 5 km and regional of order one from Bouguer anomaly are compared against vertical derivative anomaly map to see whether the shallow earth anomalies are adequately picked or not.

Total Horizontal derivative (THDR)

The horizontal gradient can be applied on the Bouguer anomaly map and this turns out to be the simplest approach to estimate contact locations of the bodies at depths. The biggest advantage of the horizontal gradient method is its low sensitivity to the noise in the data because it only requires calculations of the two first-order horizontal derivatives of the field (Phillips *et al.,* 2007).

Analytic signal (total gradient) method

The analytic signal method (Nabighian, 1972; Roest *et al.,* 1992) assumes that the sources are isolated dipping contacts separating thick geologic units. Peaks in the analytic signal amplitude, which is derived from the first horizontal and vertical derivatives of the observed gravity field, are used to locate the contacts and estimate their strike directions. If the geologic units are not thick, the depth estimates from the analytic signal method will be too shallow. The analytic signal method is moderately sensitive to noise in the data and interference effects between nearby sources. This transformation is often useful at low latitudes (e.g. this study area), particularly for the magnetic data because of the inherent problems and also with the Bouguer anomaly (GETECH, 2007). The analytic signal (AS) is the square root of the sum of the squares of the derivatives in the x, y and z directions.

$$AS = \sqrt{(\frac{\partial f_v}{\partial x})^2 + (\frac{\partial f_v}{\partial y})^2 + (\frac{\partial f_v}{\partial z})^2} \quad \text{..... (5)}$$

where $(\frac{\partial f_v}{\partial x})^2$, $(\frac{\partial f_v}{\partial y})^2$ and $(\frac{\partial f_v}{\partial z})^2$ are the squares of the first derivatives of the total gravity field in the x, y and z-directions respectively, it is very useful in locating the edges of gravity source bodies (Geosoft Oasis-montaj, 2007). The advantage of using AS technique to determine gravity dense parameters from Bouguer anomalies is the invariance of direction (inclination). The success of the AS method results comes from the fact that the location and depth of gravity sources are found with only a few assumptions about the nature of the source body, which is usually assumed as a source (for example, step, contact, horizontal cylinder or dike). For these geological models, the shape of the amplitude of the AS is a bell-shaped symmetric function located directly above the source body. We compute analytic signal inclination (ASI) as;

$$ASI = \sqrt{(\frac{\partial f_v}{\partial x})^2 + (\frac{\partial f_v}{\partial y})^2 + (\frac{\partial f_v}{\partial z})^2} \quad \text{..... (6)}$$

ASI is a measure of the depth, *D* to the source and can be estimated as in (Nabighian, 1972; Roest *et al.,* 1952);

$$D = \frac{AS}{ASI} * N \quad \text{..... (7)}$$

Where fv is the first vertical derivative of the total magnetic anomaly or gravity anomaly field, and *D* is the depth to the source body, *N* is known as a structural index and is related to the geometry of the gravity or magnetic source. For example, *N* = 4 for sphere, *N* = 3 for pipe, *N* = 2 for thin dike and *N* = 1 for magnetic contact (Reid *et al*., 1990; 2003).

Depth to basement estimation (Sedimentary thickness)

The Standard Euler deconvolution

Euler deconvolution technique is used to estimate the source depth locations of the gravity or magnetic signature in a region; and applied to profile or gridded data to solve the Euler's homogeneity equation (Thompson, 1982; Fitz-Geralda *et al.,* 2004) of the form:

$$\frac{\partial f}{\partial x}(X - X0) + \frac{\partial f}{\partial y}(Y - Y0) + \frac{\partial f}{\partial z}(Z - Z0) = N(B - f) \quad \text{..... (8)}$$

where f is the observed field at location (x, y, z) and B is the base level of the field [regional value at the point (X, X_0, Y, Y_0, Y, Y_0)] and N is the structural index or degree of homogeneity (Reid *et al.,* 1990). Source depth has been estimated based on the Euler deconvolution technique applied to the gridded data set by solving the Euler's homogeneity equation. This depth estimation depends on the type of structural index *N* which varies from –1 to 2. In the case of a gravity data set, *N* = –1 denotes the contact type bodies, *N* = 0 for thin sheet edge and thin sill dyke, *N* = 1 for cylinder, thin-bed and fault, and *N* = 2 for the point or spherical bodies. In this work, we have used N = 0, which is theoretically not accurate but provides an approximation of contact type bodies for depth calculation using the first vertical derivative of gravity data. The Bouguer gravity anomaly across the south-western part to the northwestern part shows a large deviation from local stability. The mass deficiency characterizes the sedimentary infill of the Sokoto basin. It is understood that the Sokoto basin is supposed to be overcompensated by as much as 68 mGal (Figure. 6). This combination of mass deficiency over the Sokoto basin and the excess mass over some escarpment features is due to isostatic occurrences within the strong Pan-African lithosphere. The regional correction is applied to the Bouguer gravity anomaly (Reid, 1990).

Spectral analysis technique

The spectral analysis estimates the depths to sources by making use of a statistical model which assumes the ground as an ensemble of a series of independent blocks (Spector and Grant, 1970). Various sources at different depths (deep, shallow and noise components) contribute to the cumulative response of an ensemble of sources across a given spatial frequency spectrum. The Bouguer anomaly grid was subdivided into nine (9) overlapping blocks. Each block has a dimension of about 30 by 30 km (figure. 4). The radially averaged power spectrum of the subdivided blocks was calculated and plotted. The linear segment on the spectrum is directly proportional to the depth (Naidu 1968; Spector

and Grant, 1970). The depth, *h* of an ensemble of sources is given by:

$$h = -\frac{S}{4\pi} \text{ ..... (9)}$$

where *s* is the slope of the power spectrum and *h* is the depth. The higher wavenumber portion corresponds to the shallow sources while the low wavenumber end of the spectrum corresponds to the deeper sources. The high wavenumber end of the spectrum is a consequence of noise present in the data and terrain clearance effect (Tadjou *et al.* 2009).

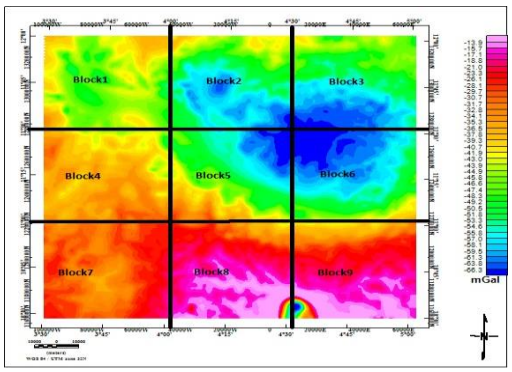

Figure 4: Blocks extracted from Bouguer gravity anomaly map (adopted from Geosoft Oasis-montaj, 2007)

RESULTS AND DISCUSSION

The residual gravity anomaly (figure. 5) is computed by removing the regional (figure. 6) effect from the complete Bouguer gravity anomaly (figure. 7).

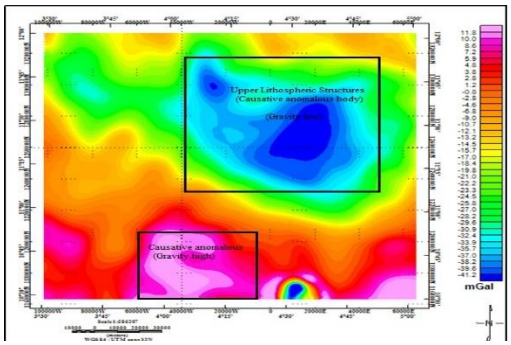

Figure 5: Residual gravity anomaly map of the Study Area

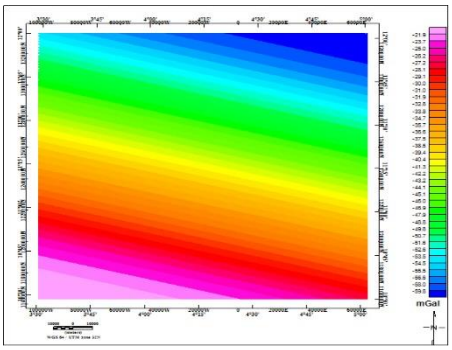

Figure 6: Regional gravity anomaly map of the Study Area

Bouguer gravity anomaly map

The Bouguer anomaly map (figure. 7) indicates lateral changes in the earth's gravity field and has a maximum anomaly value of about -13.9 mGal at the northern and northwestern parts and a minimum anomaly value of about -66.3 mGal at the southern, southeastern and southwestern parts of the study area. High gravity less negative anomalies are concentrated in the southern, southwestern and nearly the northwestern parts of the area of study. In general these gravity anomaly zones may be due to the presence of deep or thicker sediments rock. Low gravity anomalies are concentrated in the northeastern, and the northwestern parts

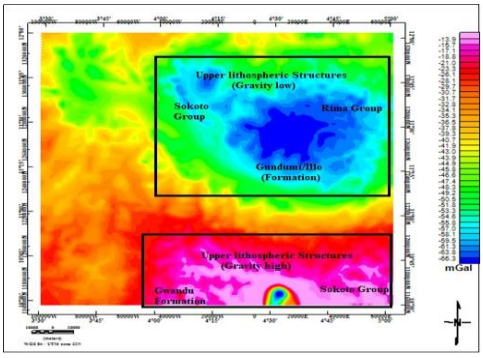

Figure 7: Bouguer anomaly Map of the Study Area.

Correlation between Free-air versus Bouguer anomaly of the Study area

The Linear regression analysis of Free-air Gravity against Bouguer anomaly was carried out from the acquired gravity data. The Bouguer reduction density was subsequently applied for recalculating the Bouguer slab corrections and the corrections for the regional terrain effects which produce the extended Bouguer Gravity map shown in (figure 7). By using the elastic thickness of the crust of 20 km and the assumed densities of the topography 2.23 gr/cc (figure 8), the crust 2.67 gr/cc and the mantle 3.07 gr/cc, suggest that the image of upper lithospheric fall within the Northeastern Region is, at present, compensated only by about 20 percent, implying the depth of the crustal root of few than 31 km (Kearey and Vine, 1990). Total compensation may be achieved when the mean value of the free-air gravity is very close to 0 mGal at which, the depth of the compensating crustal root reaches 4 km below sea level (Kearey and Vine, 1990). Free-air gravity maps are sensitive to elevation and tend to mask the deep geological bodies. The analysis of deeply seated geological features was carried out using the Bouguer gravity in which, effects of surface geology that masked the target of interest at depth were removed.

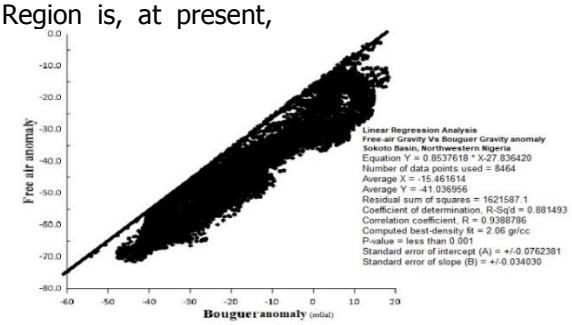

Figure 8: Plot of Linear Regression analysis of Free-air gravity versus Bouguer anomaly of the Study Area

First Vertical derivative (FVD)

The first vertical derivative (FVD) map (figure. 9) revealed sharpened edges of anomalies and shallow features, trending NW-SE. Sedimentary infill having high or low gravity anomalies are evenly distributed within the map. Similar to the residual map, the FVD map reveals shallow features with less noise and which are prominent in the northern and southern parts of the study area. Structural variations are similar to the structures observed on the residual map and dissimilar to the smoothened and broadened structures discernible on the regional map (Nabighian, 1984).

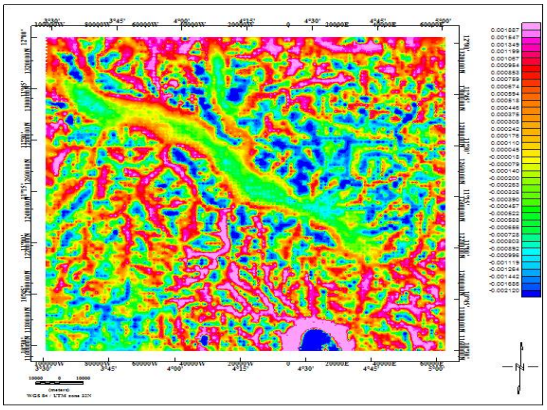

Figure: 9: First Vertical derivative anomaly map (mGal)

Total Horizontal Derivative (THDR)

The horizontal derivative transformation was utilized to decipher the contact positions of anomalous bodies at various depths. It employs the use of the first-order horizontal derivatives of the regional field. With this, a contour map displaying the depths to causative sources were generated, analyzed and used to infer the hydrocarbon potential of the study terrain. The Horizontal derivative (figure 10) allows estimation of depth, in kilometres, of a group of geologic dense body structures that vary in width, depth, and thickness, it reveals the maximum depth as occurring at the eastern end of the study area. The HDR map of the study area shows values ranging from 0.145 mGal/km to 0.219 mGal/km (figure. 10).

The maxima of HDR values are mainly located in the northeastern part of the study area where prominent ridges of Gwandu, Kalambaina, Gamba, and Gundumi formation are located and in the southern part (Kogbe, 1978, 1979, 1981). The maxima in HDR also represent the geological contacts, the interpreted contacts from HDR match known geological contacts.

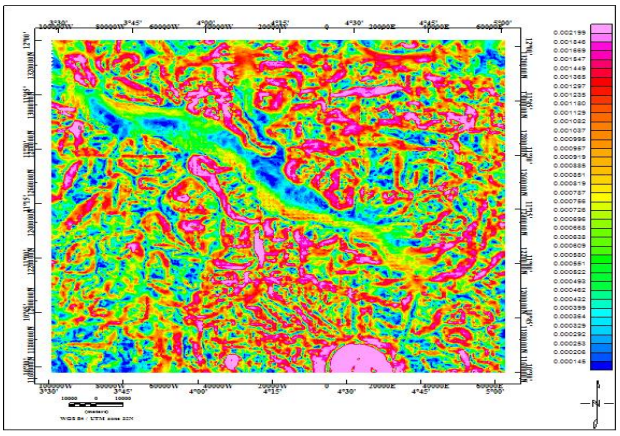

Figure: 10: Horizontal derivative of gravity data of (total gradient) (mGal)

Analytic signal

The analytic signal (AS) map is independent of the strike and dip of perturbing gravity anomalies as well as the direction of interest and represents the envelope of both the horizontal and vertical derivatives over all possible directions of the earth's gravitational field. The analytic signal (AS) transformation ensures that anomalies are positioned directly above their respective causative bodies. It does that by differentiating the total regional field gradient at each measurement point in three perpendicular directions. The mathematical basis of this transformation technique is detailed in the works of Nabighian (1972, 1984) and Roest *et al.,* (1992). High analytical amplitudes were observed at the southern and eastern sections of the map (figure.11). Locations with such large analytical amplitudes often coincide with areas of substantial limestone deposits. Presently, red moulted massive clay deposits with sandstone intercalation and ironstone are being extracted from sedimentary geological formations in Gwandu, Dange, and Dukamaje (Kogbe, 1978; 1979; 1981; Obaje *et al.,* 2020). On the other hand, low analytical signals are seen mainly at the western portion of the map, as well as at the southwestern section (figure.11). These low values are probably anomaly signatures from sedimentary in-fills.

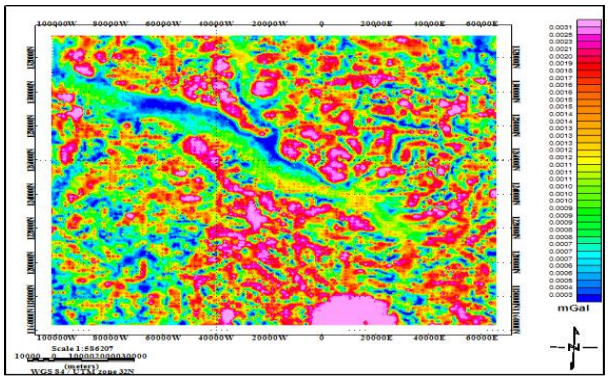

Figure 11: Analytic signal (AS) map of the study area.

Depth estimation

The Standard Euler deconvolution (SED)

In this investigation, the Euler deconvolution technique has been carried out on the gravity data. However, the available Bouguer gravity anomaly map was subjected to this method using the structural indices (0, -1, 0.5 and 1.0) and window size equal to 10, as well as a tolerance value of 7. An Euler map (figure. 12) was derived which shows clustering of circles in linear shape indicating the nature of probable contacts between the rock units. The linear clustering circles are suggestive of faults and or contacts with depth values ranging between 500 m and 5000 m for contact, and 500 m to 8000 m for dyke for all the lineaments. This gives an insight into the approximate depth range of all the lineaments/ fractures.

These solutions are trending in NW-SE, ENE-WSW, NE-SW, E-W and NNW-SSE directions (figure.12). The use of Euler deconvolution has emerged as a powerful tool for the direct determination of depth and probable source geometry in gravity data interpretations. The method can locate or outline the confined sources, dykes and contacts with remarkable accuracy. Euler deconvolution has been widely used in the automatic interpretation, because it requires no prior knowledge of the source direction and assumes no particular interpretation model (Thompson, 1982; Reid *et al.,* 1990, 2003; Stavrev, 1997). In this work, we propose to estimate both the source location and *N* using the Euler deconvolution, assuming nonlinear background. We approximate the regional field using a rational function, in which both the numerator and denominator are linear.

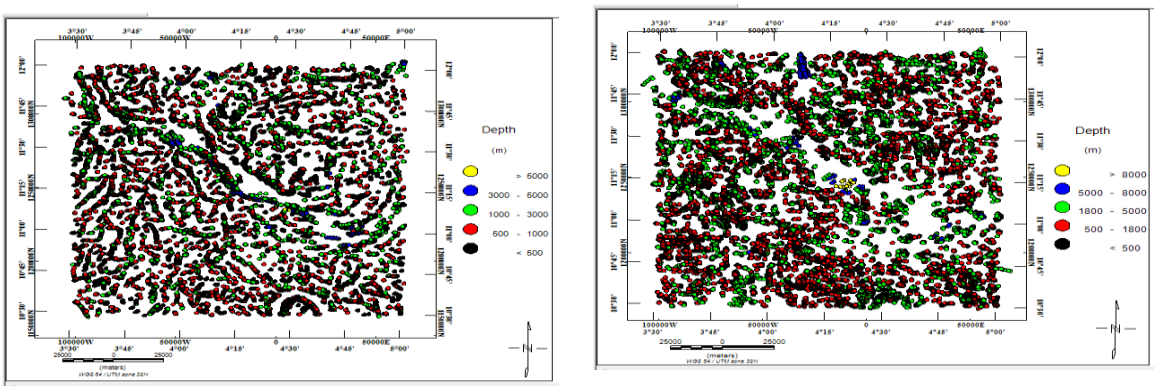

(a) **(b)**

Figure 12(a-b): Step-fault locations and their depths deduced from Bouguer gravity anomaly using Euler deconvolution for **(a)** Contact_0-7-10 and **(b)** Dyke_0.5-7-10

Spectral depth analysis

Figures 13 (a-i) show the radial power spectrum from nine (9) of the subdivided blocks (Block 1 – Block 9). The high and low-wavenumber anomalies reflect sources that are close to the surface and deep-seated, respectively. The low-wavenumber portion (layer1) which corresponds to the deep-seated sources comprises the layer of interest. The graph shows two distinct cut-off wave numbers (cyc/km) of the power spectrum trends, along with the indicated depth to the corresponding infill boundaries. The first layer consists of deep spectrum values with the best line fit as d_i = 3.908 km, 5.352 km, 4.123 km, 3.07 km, 2.894 km, 5.016 km, 5.366 km, 3.686 km and 4.247 km corresponds to the depth of the top of intrusive structures. The second layer indicates the shallow depth values of the spectrum with the best line fit *di* = 1.540 km, 2.564 km, 2.413 km, 0.770 km, 0.769 km, 0.1696 km, 1.986 km, 1.629 km and 1.742 km with correspond to the depth of metalliferous ore bodies (figure. 13 (a-b)). These depth estimate values were subsequently used for the constraint to the correlation of interpretation of Euler deconvolution. The average depths estimated from the subdivided blocks were compiled to generate 2D and 3D depth maps (figure. 14 (a–b)) of the study area. The 2D and 3D depth maps both show a relatively deep and shallow region (curved area) with sedimentary thicknesses/depth to the basement ranging between 2.0 and 7.5 km in the south-eastern part of the study area. Away from this zone, a lower average sedimentary thickness range (< 3.25 km) was observed in the study area. The 3D surface map of the basement comprises a series of depressions and uplifts (Figure.14b), a typical representation of fold features. These folds are thought to have been formed during the tectonic event that affected the study area in Cenomanian and Santonian times, which led to the (slight brittle and) intense ductile deformation of the basement surface (Kogbe, 1972, 1979, 1981; Petters & Ekweozor, 1982). The computed depth values can imply the hydrocarbon potential of the study area. An average sedimentary depth of about 4.18 km compares satisfactorily well with previous literature and implies that the area is favourable for the formation and accumulation of hydrocarbon given other factories for a petroleum system. According to Gluyas and Swarbrick (2005), an average sediment thickness of about 3 – 4 km is required for the accumulation and entrapment of hydrocarbon. Only the southwestern end and northeastern part of the study area revealed sediment thickness up to 4 km. In addition, the presence of numerous intrusive structures at varying depths signifies a high-temperature environment, which reduces the possibility of hydrocarbon presence. The potential source rocks within the study area would have been broiled beyond the hydrocarbon-generating window, although, the study area possesses immense potential for metalliferous ore deposits.

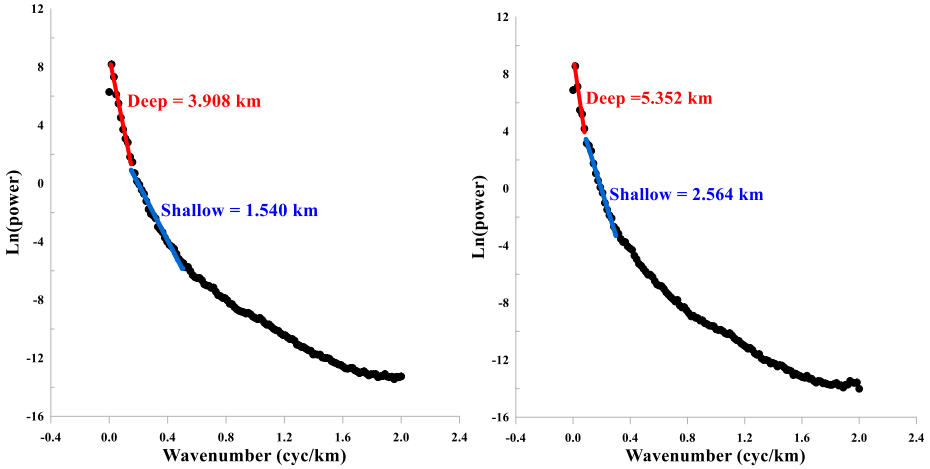

(a) Block 1 **(b) Block 2**

Figure. 13 (a-b): A spectral plot an example from nine of subdivided blocks

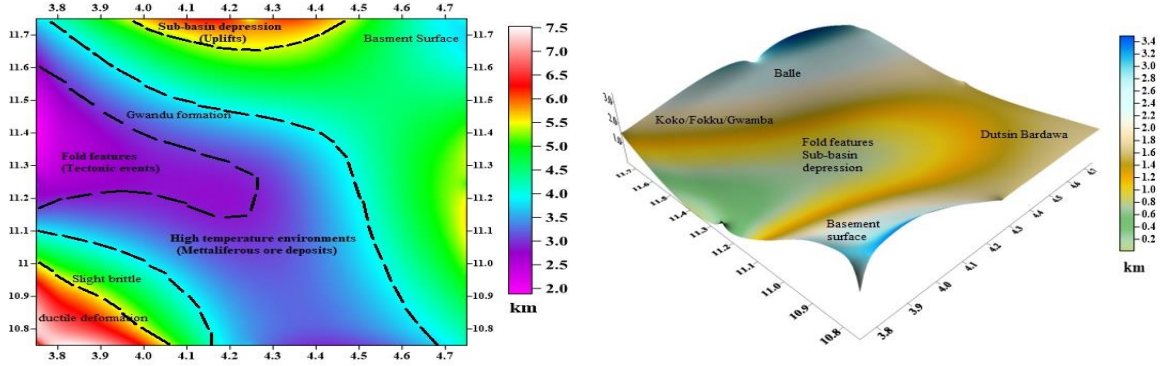

(a) **(b)**

Figure 14: Depth map obtained from spectral analysis method in **(a)** 2D spectral depth map (deep-seated features > 4.00 km) and **(b)** 3D depth map (shallow features < 4.00 km)

CONCLUSION

In this study, the acquired satellite gravity data have been analysed and interpreted using a combination of enhanced mathematical techniques so that updated information about structural features for concealment of Hydrocarbon accumulation or related mineralizations, edges, lineaments, trends and depth of the gravity source responsible for potential lithological structures in some parts of the Sokoto Basin of northwestern Nigeria were revealed. The separation of regional residual anomaly map reveals variations and distributions of anomalies at various sizes concealed as shear and weak zones characterized by positive and negative (high and low) gravity anomalies values-trending majorly in NW-SE and E-W direction. The interpretation of the results in the study area also reveals the varying amplitudes of the anomaly signature which implies that the gravity source body is not evenly distributed across the study area. The region of low gravity anomaly values from the Bouguer anomaly map suggest possible discontinuity or faults or fractures, whereas the region with high gravity anomaly, less negative indicate that the area underlain with iron deposited mineral or escarpment features/ridges. The estimated depths vary between 2.0 km and 7.0 km which suggest that the gravity source body suspected to be 3.25 km is a near-surface feature. The local geological mapping of the study area revealed that the area is underlain mainly by red moulted iron, sandstone intercalation, ironstone phosphatic nodules, limestone and carbonaceous mudstone. Results showed that the application of potential fields in particular satellite gravity data was successful in imaging the upper lithospheric structures and estimating the depth to the causative bodies of the sedimentary infill in some parts of the Sokoto Basin.

Acknowledgements

The acquisition of the satellite gravity data was supported and downloaded from the United State Geological Survey, USGS, website. We thank colleagues from Ahmadu Bello University Zaria and the State Ministry of Environment and Solid Mineral of Sokoto, Kebbi and Zamfara States of Nigeria, for providing insight and expertise that greatly assisted this research and for comments that greatly improved the manuscript.

Funding statement

This research did not receive any specific grant from funding agencies in the public, commercial, or not-for-profit sectors.

Disclosure statement

No potential conflict of interest was reported by the author(s).

REFERENCES

Ali, M, Halidu, H, and Mijinyawa, A. (2016) Stratigraphic Review of the cretaceous Tertiary Deposits of the Iullemmeden Basin in Niger and Nigeria. Asian Journal of Applied Sciences (ISSN: 2321 – 089), Vol. 4(2) www.ajouronline.com.

Askari, A., (2014). Edge detection of gravity anomaly sources via the tilt angle, total horizontal derivative, total horizontal derivative of the tilt angle and new normalized total horizontal derivative. Scholars J. Eng. Technol 2 (6B), 842-846.

Balmino, G., Vales, N., Bonvalot, S., Briasis, A., (2011). Spherical harmonic modelling to ultra-high degree of Bouguer and isostatic anomalies. J. Geodes. 86, 499-520. http://dx.doi.org/10.1007/s00190-011-0533-4.

Charles, C.U., Innocent, J.A., and Chiduben, O.E., (2020). Analysis of Aeromagnetic Data of Ikwo and Environs, Southeastern Nigeria: A Mineral and Hydrocarbon Exploration Guide. Natural Resources Research © 2020, https://doi.org/10.1007/s11053-020-09633-3, International Association for Mathematical Geosciences.

Fairhead, J. D., and Okereke, C. S. (1988). A regional gravity study of the West African rift system in Nigeria and Cameroon and its tectonic interpretation. Tectonophysics, 143,141–159.

Fitz Geralda, D., Reid, A., and McInerneya, P. (2004). New discrimination techniques for Euler deconvolution. Computers & Geosciences, 30: 461-469.

Gluyas, J., and Swarbrick, R. (2005). Petroleum Geoscience. Oxford: Blackwell Science.

Gunn, P.J., FitzGerald, D., Yassi, N. (1997). Complex attributes: new tools for enhancing aeromagnetic data. Aust Geol Surv Organ Res 25:16–17.

Hesham, S.Z., and Oweis, H.T. (2016). Application of High – pass Filtering Techniques on Gravity and Magnetic Data of the Eastern Qattara Depression Area, Western, Desert, Egypt. NRIAG. Journal of Astronomy and Geophysics, Vol. 5(1); 106 – 123. www.elsevier.com/locate/nrjag

Hinze William, J., Von Frese, Ralph R.B., Saad, Afif H., (2013). Gravity and magnetic exploration Principles, Practices, and Applications. Cambridge university press.first published 2013.

Ismail, A.M., Sultan, S.A., Mohamady, M.M., (2001). Bouguer and Total Magnetic Intensity maps of Sinai Peninsula, Scale 1: 500,000. In: Proc. 2nd International Symposium on Geophysics, Tanta, pp. 111–117.

Jacobsen, Bo Holm, (1987). A case for upward continuation as a standard separation filter for potential-field maps. Geophysics 52 (8), 1138–1148.

Kebede, Hailemichael, Alemu, Abera, Fisseha, Shimeles, (2020). Upward continuation and polynomial trend analysis as a gravity data decomposition, case study at ziway-shala basin, central main Ethiopian rift. Heliyon 6 (1), e03292.

Keary, P. and Vine F.J., (1990). Global Tectonics, Blackwell Scientific Publications, pp.36-37.

Kogbe, C. A., (1972). Geology of the Upper Cretaceous and Lower Tertiary sediments of the Nigerian Sector of the Iullemmeden Basin (West Africa), *Geologische Rundschau,* Vol. 62(1), pp. 197-211, Stuttgart.

Kogbe, C. A., (1979). Geology of southeastern portion of the Iullemmeden Basin (Sokoto Basin), *Bull.* Dept. Geology, Ahmadu Bello University, Zaria, Nigeria, 2, 420p.

Kogbe, C. A., (1981). Cretaceous and Tertiary of the Iullemmeden Basin in Nigeria (West Africa), *Cretaceous Research* **2**, 129 – 186.

Linsser, H., (1967). Investigation of tectonics by gravity detailing. Geophys. Prospecting. 15, 480–515.

Mammo, T., (2004). Mapping the crustal-mantle boundary beneath the Afar Depression. Gondwana Res. 7, 855-861. http://dx.doi.org/10.1016/S1342-937X(05)71069-8.

Mammo, Tilahun, (2010). Delineation of sub-basalt sedimentary basins in hydrocarbon exploration in north Ethiopia. Mar. Petrol. Geol. 27 (4), 895–908.

Mickus, Kevin L., Carlos, L.V., Aiken, Kennedy, W.D., (1991). Regional-residual gravity anomaly separation using the minimum-curvature technique. Geophysics 56 (2), 279–283.

Nabighian, M. N. (1972). The analytic signal of two-dimensional magnetic bodies with polygonal cross-section: Its properties and use for automated anomaly interpretation. Geophysics, 37,507–517.

Nabighian, M. N. (1984). Towards a three-dimensional automatic interpretation of potential field data via generalised Gilbert transforms: Fundamental relations. Geophysics, 49,780–789.

Naidu, P.S., (1968). Spectrum of potential field due to randomly distributed sources. Geophysics 33:337–345.

Nettleton, L. L. (1976).Gravity and magnetic in oil prospecting. New York: McGraw-Hill.

Oasis Montaj Program v.8.4, 2015. Geosoft mapping and processing system, version 8.4, 2015.

Obaje, N. G., Faruq, U.Z., Bomai, A., Moses, S.D., Ali, M., Adamu, S., Essien, A., Lamorde, U., Umar, M.U., Ozoji, T., Okonkwo, P., Adamu, L., and Nda, I.A. (2020). A Short Note on the Petroleum Potential of the Sokoto Basin in Northwestern Nigeria. *Petroleum Science and Engineering.* **4** (1), 34-38.

Obaje, N.G. (2009). The Benue Trough Geology and Mineral Resources of Nigeria. Springer, Dordrecht Heidelberg, New York, London P.57 ISBN 3-540-92684-4.

Obaje, N.G., Wehner, H., Abubakar, M.B., Isha, M.T. (2009). Nasara- I will, Gongola basin Benue Trough Nigeria; source-rock evaluation. Journal of Petroleum, 27 (2), 191-206.

Olawale, O.O., Moroffdeen, A.A., and Oluwatoyin, A.A. (2020). Structural Interpretation and Depth Estimation from Aeromagnetic Data of Abigi-Ibebu-waterside area of Eastern Dahomey Basin, Southwestern Nigeria. Geofisica International, Vol. 58 (4) pp 29-37, Science. ISSN 0016-7169.

Petters, S.W., Ekweozor, C.M. (1982). Petroleum geology of Benue Trough and southern Chad Basin Nigeria. AAPG Bull 66:1141–1149

Phillips, J.D., R.O. Hansen, and R.J. Blakely (2007). The use of curvature in potential-field interpretation, Explor. Geophys. 38, 2, 111-119, DOI: 10.1071/ EG07014.

Reid, A.B., (2003). Short note: Euler magnetic structural index of a thin bed fault. Geophysics, Published electronically,

Reid, A.B., J.M. Allsop, H. Granser, A.J. Millett and I.W. Somerton, (1990). Magnetic interpretation in three dimensions using Euler deconvolution. Geophysics, 55: 80-91.

Reid, A.B.D. Fitz Gerald and P. McInerney, (2003). Euler deconvolution of gravity data. SEG Annual Meeting, Dallas, accepted for presentation.

Roest, W. R., Verhoef, J., and Pilkington, O. (1992). Magnetic interpretation using the 3D analytic signal. Geophysics, 57, 116–125.

Spector A, and Grant F (1970). Statistical models for interpreting aeromagnetic data. Geophysics 35:293–302.

Stavrev, P.Y., (1997). Euler deconvolution using differential similarity transformations of gravity or magnetic anomalies. Geophys. Prosp.45, 207–246.

Sultan, A.S.A., Mohammed, E., Abou, H.M., Mahmoud, M., Ismail, E., Ahmed, K., Enas, M.A. (2018). Implementation of magnetic and gravity methods to delineate the subsurface structural features of the basement complex in central Sinai area, Egypt. NRIAG Journal of Astronomy and Geophysics, vol. (7) pp 162 – 174. Journal homepage: www.elsevier.com./locate/nrjag.

Tadjou, J.M, Nouayou, R., Kamguia, J., Kande, H.L., Manguele-Dicoum, E. (2009). Gravity analysis of the boundary between the Congo Craton and the Pan-African belt of Cameroon. Aust J Earth Sci 102:71–79.

Tiberi, C., Ebinger, C., Ballu, V., Stuart, G., Oluma, B., (2005). Inverse models of gravity data from the Red Sea-Aden-East African rifts triple junction zone. Geophys. J. Int. 163, 775-787.

Topex.ucsd.edu, Extract topography or gravity data from global 1 – minute grids in ASCII XYZ-format.

Tselentis, G., Drakopoulos, J., Dimitriadias, K., (1988). A spectral approach to Moho depths estimation from gravity measurements in Epirus (New Greece). J. Phys. Earth 36, 255-266. https://doi.org/10.4294/jpe1952.36.255.

Thompson, D.T.T., (1982). Euler, a new technique for making computer assisted depth estimates from magnetic data. Geophysics V. 47, 31–37.

Thurston, J.B, Smith, R.S. (1997). Automatic conversion of magnetic data to depth, dip, and susceptibility contrast using the SPI method. Geophysics 62(3):807–813.

Thurston, J.B. Smith, R.S. (1997). Automatic conversion of magnetic data to depth, dip, and susceptibility contrast using the SPITM method, Geophysics 62 (3) 807–813.

Zelalem, D., Kevin, M., David, B., Mohammed, G.A., Estella, A., (2018). Upper lithospheric structure of the dobi graben, Afar Depression from magnetic and gravity data. J. African Earth Sciences, 147, 136-151. https://doi.org/10.1016/j.afrearsci.2018.06.012.